ELSEVIER

Cognitive Brain Research 4 (1996) 39–47

COGNITIVE BRAIN RESEARCH

Research report

Non-invasive detection of neuronal population activity in human hippocampus

C.D. Tesche [a,*], J. Karhu [b], S.O. Tissari [a,1]

[a] Low Temperature Laboratory, Helsinki University of Technology, Espoo 02150, Finland
[b] Department of Clinical Neurophysiology, Kuopio University Hospital, Kuopio, Finland

Accepted 11 October 1995

Abstract

Medial temporal brain structures and hippocampus are associated with memory encoding and activate during registration and transfer of information within cortico-hippocampal circuits. Hippocampal dysfunction may cause learning and memory deficits as well as epileptogenesis. We monitored neuronal population activity of the human hippocampal formation with a whole-head magnetoencephalographic array. Attention-dependent hippocampal responses were elicited by auditory oddball stimuli. The most prominent responses emerged 200–500 ms after attended oddballs in good agreement with earlier intracranial recordings. Some activation of hippocampal source areas was seen at 60–100 ms. This completely non-invasive method permits access to cortico-hippocampal neural networks on the millisecond time scale during normal and abnormal brain activation and thus provides a new tool for evaluation of cognitive processes and pathological conditions involving hippocampal formation.

Keywords: Hippocampus; Human; Medial temporal lobe; Functional brain imaging; Magnetoencephalographic (MEG) source mapping; Auditory evoked response; Signal-space projection (SSP)

1. Introduction

In everyday life, rapid and accurate exchange of information between sensory cortical areas and hippocampal structures is essential for comparison of novel input with stored memory traces and for binding related fragments with each other [31,41]. Memory encoding and medial temporal brain structures were initially associated by studying a single case of human amnesia with a bilateral, operative destruction of amygdala and hippocampus [32]. Ablations of hippocampus and amygdala in monkeys were followed by an impaired ability to recognize familiar objects [23] and to form associations between stimuli [24,25]. Recent studies suggest that main hippocampal input and output routes which are embedded in entorhinal and parahippocampal cortices are equally crucial to memory functions [34,43].

Hippocampal activation in tasks which depend on short-term or 'working' memory has been demonstrated with PET in man [19,27] and in monkeys [4], and diminished hippocampal volumes in MRI seem to accompany memory disorders [29,35]. Tasks which require sustained attention [27], such as the detection of an oddball target from a sequence of standard stimuli, also activate the hippocampus. Depth electrode and electrocorticography recordings in epileptic patients utilized for the localization of epileptogenic areas prior to epilepsy surgery have revealed event-related responses (ERPs) to attended infrequent stimuli in the medial temporal lobe [6], including task-dependent ERP responses to auditory, visual and somatosensory oddballs at peak latencies of 300–600 ms [20,36].

In scalp electroencephalographic (EEG) recordings, ERPs at 300–600 ms (P300) are proposed to reflect the sustaining and updating of models of the external environment [3,39]. EEG measurements provide non-invasive detection of current flow in neuronal populations at arbitrary depth with good temporal resolution. However, the identification of hippocampal activity from EEG recordings has been problematic. In particular, bilateral damage to or removal of hippocampal formation and medial temporal tissue has been reported with no apparent impact on scalp

* Corresponding author. Fax: (358) (0) 451-2969; E-mail: tesche@neuro.hut.fi

[1] Present address: Picker Nordstar Ltd., Helsinki, Finland.

0926-6410/96/$15.00
SSDI 0926-6410(95)00044-5

ERPs [13,28]. Widespread patterns of electric activity on the scalp may be generated by relatively localized sources by the impedance mismatch between scalp, skull and brain. If many cortical generators are active during cognitive processing [5,42], the overlap of the EEG patterns makes it difficult to identify subcortical contributions. This problem impairs study of the dynamics of the interaction between neural networks in sensory cortical areas and medial temporal lobe structures which are involved in perception and subsequent memory encoding in normal subjects.

Magnetoencephalographic (MEG) arrays of superconducting sensors located over the scalp record neuronal population activity with the same excellent temporal resolution as EEG. MEG arrays are frequently used to identify source areas for localized population activity, particularly within superficial cortex (for a review, see [7]). Since MEG signals are not affected by the skull, the identification of multiple cortical generators is facilitated by the relatively limited overlap of the magnetic field patterns.

Several previous studies performed with MEG arrays with partial head coverage have suggested generators of evoked magnetic responses to oddball stimuli in deep source areas, including hippocampus [12,26], medial temporal lobe [16] and thalamus [30]. Most of these studies have relied on the detection of characteristic double-lobed patterns of magnetic responses produced by localized sources. However, this approach requires responses which are temporally isolated from more widespread cortical activity. Thus, although dipolar patterns have been observed [26], the determination of task-dependent waveforms for activity within hippocampal formation has been difficult. The introduction of whole-scalp MEG arrays with the capacity to record simultaneously multiple sources of activity provides a unique opportunity for the investigation of the dynamics of hippocampal population responses, provided that a methodology for the separation of medial temporal and deep sources from more superficial cortical activity can be developed.

2. Materials and methods

We recorded neuronal population responses to interspersed auditory and visual oddball stimuli non-invasively with a whole-head MEG array [1]. The use of both visual and auditory modalities provided the opportunity to study auditory responses during a task with a relatively challenging cognitive load and to obtain functional localization of all primary sensory cortices. In this study, the use of the whole-head MEG array eliminated the effects of intertrial variability on source localization, facilitating the identification of attention-dependent widespread activity generated by deep sources. We extend conventional MEG analysis techniques for the characterization of superficial sources to include responses generated by medial temporal and deep sources. In particular, signal-space analysis (SSP) [10,38] is utilized to disentangle activity within hippocampal source areas from other cortical generators of the magnetic evoked response. A preliminary report of this work has appeared in abstract form [37].

2.1. Subjects and experimental conditions

Four healthy subjects (3 males; aged 29–50 years) were asked to select an auditory oddball target in a flow of randomly presented auditory and visual stimuli (binaural tone bursts of 50 ms duration, 75% at 1 kHz and 25% at 2 kHz, and centrally presented colored squares of 50 ms duration, 75% green and 25% red, at random interstimulus intervals of 0.15–0.3 s). Stimuli were observed passively or with instruction given at the beginning of the stimulus block for an imperative to execute a motor response.

Subjects were seated inside a magnetically shielded room after providing informed consent. Magnetic field responses evoked by the stimuli were recorded non-invasively over the scalp with a helmet-shaped array of 122 superconducting SQUID magnetometers (Neuromag-122™). In this system, a superficial current dipole source flowing tangent to the skull produces a maximum signal in sensors located directly above the source. The data were sampled at 400 Hz, bandpass filtered at 0.03–130 Hz and averaged on line. The vertical electro-oculogram was used to reject data contaminated by eye movements and blinks.

2.2. Characterization of superficial sources

It is not possible to calculate underlying neuronal source activity directly from MEG signals without additional constraints on the current flow [9]. Source distributions which are consistent with the data may be determined by comparing the field patterns calculated for a specific configuration with those measured by the array. Equivalent current dipole (ECD) sources [2] are frequently used to represent localized sources of activity which are believed to generate early auditory evoked responses to stimuli and sensorimotor responses synchronized to movement in cortex. ECD sources approximate activation of neuronal populations within cortical areas of several cm with a short flow of current parametrized by location and orientation. In this study, ECD source parameters for responses in temporal, occipital and somatosensory cortex were determined from a least squares fit between simulated field patterns and the MEG data (for a review, see [7]). Noise-free field patterns for these sources which were used in subsequent analysis of the data were then generated by forward modeling using a spherical model for the head.

2.3. Characterization of deep sources

We used a realistic head model based on individual subject MRIs to forward model fields generated by neuronal current flow located in and near the hippocampus. Current flow was separated into 3 orthogonal components: a source h_a oriented predominantly in the anterior–posterior direction of hippocampus, source h_c confined to the coronal plane at approximately 45° with respect to the vertical and a nearly radial source, h_r. The magnetic field arising from medial temporal sources were calculated using a single-compartment boundary-element conductor model for the head [8]. The geometry of the cranial volume utilized in the calculation was extracted from each subject's MRI images.

2.4. Signal-space projection

SSP [10,38,40] was used to combine the analysis of responses generated by medial temporal areas with those from more superficial cortex. In SSP, current distributions in the brain are characterized by the signals which they generate in the array of N sensors. Thus both the current sources in the brain and the signals which they generate in the array are described by vectors in a common N-dimensional vector space. A component of the signal is a pattern of responses with a fixed spatial distribution or topography whose overall amplitude may vary in time. The total MEG signal

$$\mathrm{M_T}(t) = \sum_{i=1}^{N} a_i(t)\mathrm{s}_i + \mathrm{n}(t)$$

where the unit vectors s_i are parallel to the vectors determined by the spatial distributions of each component and the waveforms $a_i(t)$ describe the time dependencies of the amplitudes of each component. The term $\mathrm{n}(t)$ includes intrinsic system noise and may also include responses from current flow within the brain which are not explicitly modeled as components. Waveforms determined from a pseudoinverse of the matrix $(\mathrm{s}_1, \mathrm{s}_2, \ldots, \mathrm{s}_N)$ give an unbiased estimate for the activity of each component when $\mathrm{n}(t)$ consists of spatially uncorrelated and normally distributed noise (for a more complete description see [38]).

2.5. SSP waveform scaling

SSP components may be determined from the field patterns generated by localized or distributed current flow in the brain. Components for well-localized sources may be parametrized by an ECD location and orientation. Although ECD locations may be determined from MEG data with an accuracy of a few mm [21], the magnetic field pattern may reflect neuronal population activity within a much wider area. Moreover, simulations indicate that both conventional multi-dipole model and SSP waveforms may contain contributions from simultaneously active neighboring sources separated by distances on the order of cm or more [18,40].

In the present study, we used SSP to generate waveforms for components which were specified by ECD sources within the hippocampus. The location of the ECDs were determined from the subject's MRI. Since the source locations were fixed, inadequately modeled activity in cortical or adjacent subcortical sources would be reflected in extraneous contributions to the SSP waveform, rather than in a poor goodness-of-fit of the data to a particular dipolar field pattern. The possible existence of extraneous contributions was searched for by observing how the SSP waveform changed as the ECD was moved from one location to another in the neighborhood of the hippocampus. This family of displaced ECD sources and the SSP waveforms which they determine were used to 'probe' the

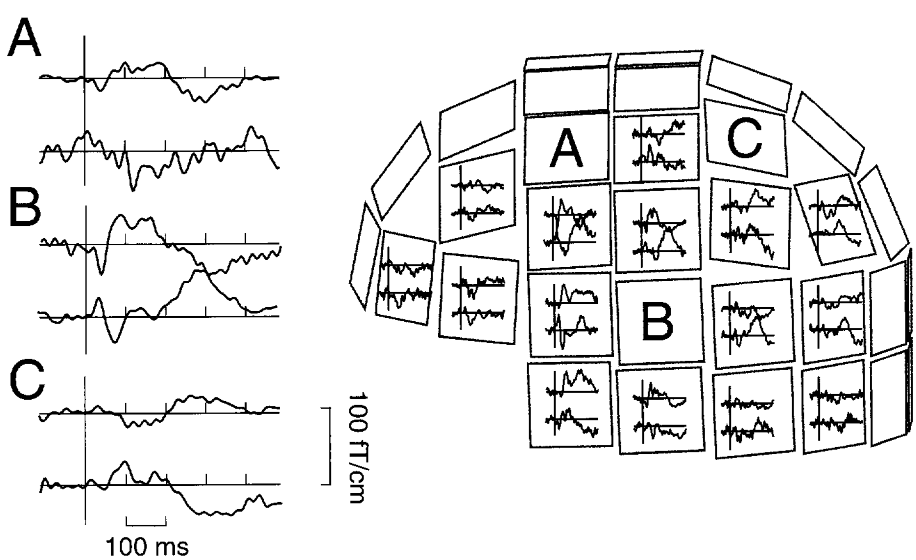

Fig. 1. Examples of average magnetic signals (167 responses) for subject S1 evoked by the auditory oddball stimuli. The subject lifted the right index finger on the presentation of the oddball (reaction time 0.35 s). Data recorded for 100 ms preceding and 500 ms following the auditory oddball are shown at the location of the sensors on the left side of the helmet-shaped array. The back of the head is on the right.

consistency between the predictions of a given source model and the results computed from the data. SSP unit vectors s_k were determined from forward modeling for each displaced ECD 'probe'. Waveforms for each ECD probe were then computed from the data. MEG system noise was computed for each ECD probe by applying the SSP algorithm to data recorded without the subject.

Numerical simulations of field patterns determined by a family of 'test' ECD sources located in the neighborhood of the hippocampus were performed using realistic models for each subject's head. SSP waveforms for each ECD probe were then computed from the simulated data. For simplicity, the same locations were used for both the 'probe' ECDs and the 'test' ECDs. The pattern of responses for the probes determined from the data were compared for consistency (within $\pm\sigma$ of the system noise) with those determined from the numerical simulations. Inconsistencies between the simulated and measured results may be generated by either a distribution of sources in the neighborhood of the hippocampus, or by distant sources which are insufficiently modeled as other components. This analysis gave a local measure for the fit between the simulation and data, rather than the global measure used in conventional least-squares fitting algorithms.

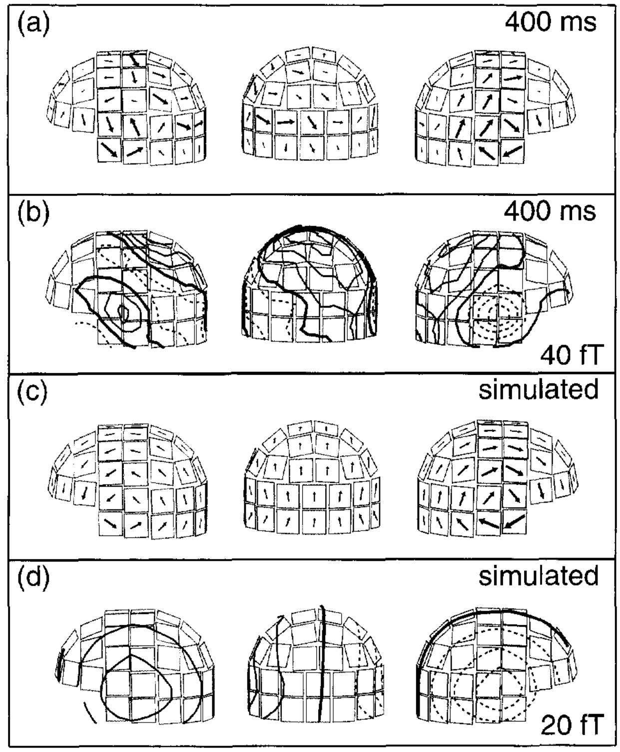

Fig. 2. a: magnetic field gradients for evoked response data recorded 400 ms after the presentation of the auditory oddball for subject S2. The subject lifted the right index finger on the presentation of the oddball (reaction time 0.35 s). The arrows indicate the direction in the plane of the sensors of the gradients of the component of the magnetic field normal to the sensor coils. The amplitudes scale with the lengths of the arrows. b: contour map of the normal component of the magnetic field. The contour spacing is 40 fT. Simulated magnetic field (c) gradients and (d) contours for simultaneous activation of a 10-nA source located in the left anterior hippocampus and a 5-nA source located in right anterior hippocampus with current flow in the posterior direction. The contour spacing is 20 fT.

3. Results

Fig. 1 shows a subset of the MEG response evoked by attended auditory oddball stimuli. Sensors located over the temporal lobe (B) recorded evoked responses reflecting processing of auditory information at 35 and 85 ms. In contrast, widespread MEG activity is evident at 200–500 ms, particularly over (A) sensorimotor, (B) temporal, and (C) parietal areas. The waveforms are quite different even between adjacent planar gradiometer sensors.

Fig. 2a and b show magnetic field topographies recorded by the array 400 ms after the attended auditory oddballs. Fig. 2c and d show simulated magnetic field data for neuronal population activity in anterior hippocampus. The topographies are shown both as arrow maps determined directly from the data and as magnetic field contours calculated from a spherical model for the head. The arrow map in Fig. 2a shows a relatively widespread pattern of activity in sensors located over the right hemisphere. In contrast, the pattern of arrows over the left hemisphere is more complex. The planar gradiometer sensors in the array record a maximum signal directly over a localized source. As the separation between a source and sensor array is increased, adjacent sensors begin to detect a regular pattern of responses. Thus the pattern of arrows over the right hemisphere is suggestive of a deep source within the right hemisphere, whereas the pattern of arrows over the left hemisphere is suggestive of multiple superficial sources within the left hemisphere.

An example of an arrow map for an ECD source h_a located in right anterior hippocampus is shown in Fig. 2c. This source produces a relatively smooth pattern in the gradient data which resembles that recorded over the right hemisphere in Fig. 2a. The simulated magnetic field contours (Fig. 2d) exhibit widely spaced extrema located over the temporal areas. These contours represent magnetic field lines which emerge from the right temporal area, circle around the head and re-enter the figure over the left temporal area. In free space, magnetic field lines coil symmetrically around ECD sources. Thus widely spaced contours are indicative of deep sources. However, the reconstruction of magnetic field contours using a spherical head model from data or from simulations performed using realistic head model leads to a distortion of the field contours and thus of the apparent dipole location. All source modeling is performed on the original gradient data and gradient pattern simulations.

Additional activity is apparent in the data in sensors located over the left parietal, occipital and sensorimotor areas compared to that present in the simulations. This suggests that a complex set of sources was active within more superficial cortical association areas at 400 ms. Thus, the determination of hippocampal waveforms at these latencies must involve the detection of medial temporal activity in the presence of the simultaneous activation of several other source areas. Moreover, the identification of activity within hippocampal source areas with this technique does not preclude the existence of other cortical generators of the P300 responses observed in the waveforms recorded by the sensors [42].

Fig. 3 shows waveforms determined from a multi-source SSP analysis. ECD source locations and orientations in the left and right supratemporal auditory cortex (Fig. 3a) were determined separately 85 ms after the auditory oddball stimuli from subsets of sensors located over each temporal area. Movement-related responses triggered on the lifting of the finger were used to determine a third ECD source in the contralateral sensorimotor area (Fig. 3b). ECD sources were also located in anterior hippocampus to probe medial temporal responses (Fig. 3c). More complex topographies describing visual evoked responses triggered on the visual stimuli at 126 and 164 ms were included in the analysis. The activity of these sources following auditory oddball stimuli was negligible and is not shown in the figure. The temporal order of the activation of the cortical and medial temporal sources is shown in the waveforms in Fig. 3d–h. Initial responses in the left and right auditory areas are prominent at 35 and 85 ms after the auditory stimuli. The most prominent responses in the hippocampal waveforms appear 200–500 ms after the attended oddballs, with some activation also at 60–140 ms.

Fig. 4 illustrates the application of waveform scaling to test the consistency between the results of the SSP analysis and numerical simulations of hippocampal activity. SSP waveforms were calculated for 'probe' ECDs located at sites A–E as indicated on the approximately coronal MRI image in Fig. 4a. Site C coincides with the location of h_a.

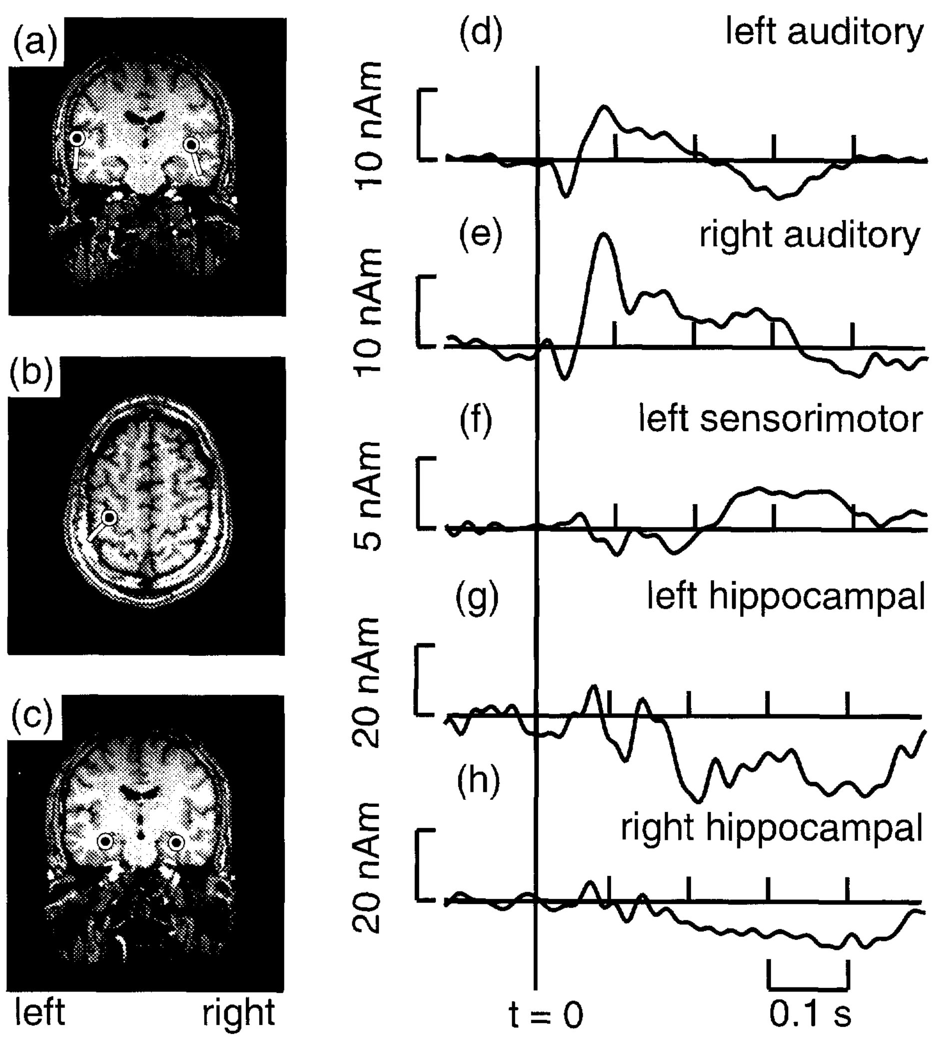

Fig. 3. Location on MRI images of equivalent current dipole sources in the left and right supratemporal auditory cortex (a), left sensorimotor area (b) and left and right anterior hippocampus (c). d–h: signal-space projection waveforms for evoked responses to auditory oddballs. The subject lifted the right index finger on the presentation of the oddball (reaction time 0.35 s). The current flow in g and h is in the anterior direction.

The waveform for the evoked response to auditory oddballs for component h_a is shown in Fig. 4b. Uncorrelated system noise, which is added onto the h_a waveform, is shown as a simulated noise waveform. The standard deviation of the system noise is shown as a shaded horizontal band. Good signal-to-noise for the SSP waveform is apparent near 80 and 100 ms and at 200–500 ms after the auditory oddball, even though the source location for h_a is 5 cm below the scalp. Spontaneous activity, particularly in the α-band, has been suppressed by the visual stimuli and the affects of attention to the point that baseline fluctuations in the waveform are on the order of the system noise.

Simulated responses for a set of 'test' ECD sources in the neighborhood of the hippocampus are shown in Fig. 4c. Magnetic field patterns were computed from a realistic head model for an ECD source of uniform magnitude located at one of the sites A–E (indicated by the letters on the horizontal axis). The pattern of responses in the family of 'probe' ECDs was then computed for each 'test' source. For example, the largest difference between the 'probe' responses occurs for the deepest 'test' source E.

The pattern of activity in the 'probe' responses computed for the simulated data are compared with those determined by the evoked response data in Fig. 4d. Responses computed from the data that are within $\pm\sigma$ of the simulated values are indicated by the unshaded epochs. For example, the waveform amplitudes increase with the depth of the 'probes' at 200–400 ms, but are almost independent of the 'probe' locations at $t = 0$. At 400 ms the waveform scaling is exactly consistent with that computed from the simulation for an isolated ECD source h_a at site C. In contrast, the shaded epochs in Fig. 4b and d indicate

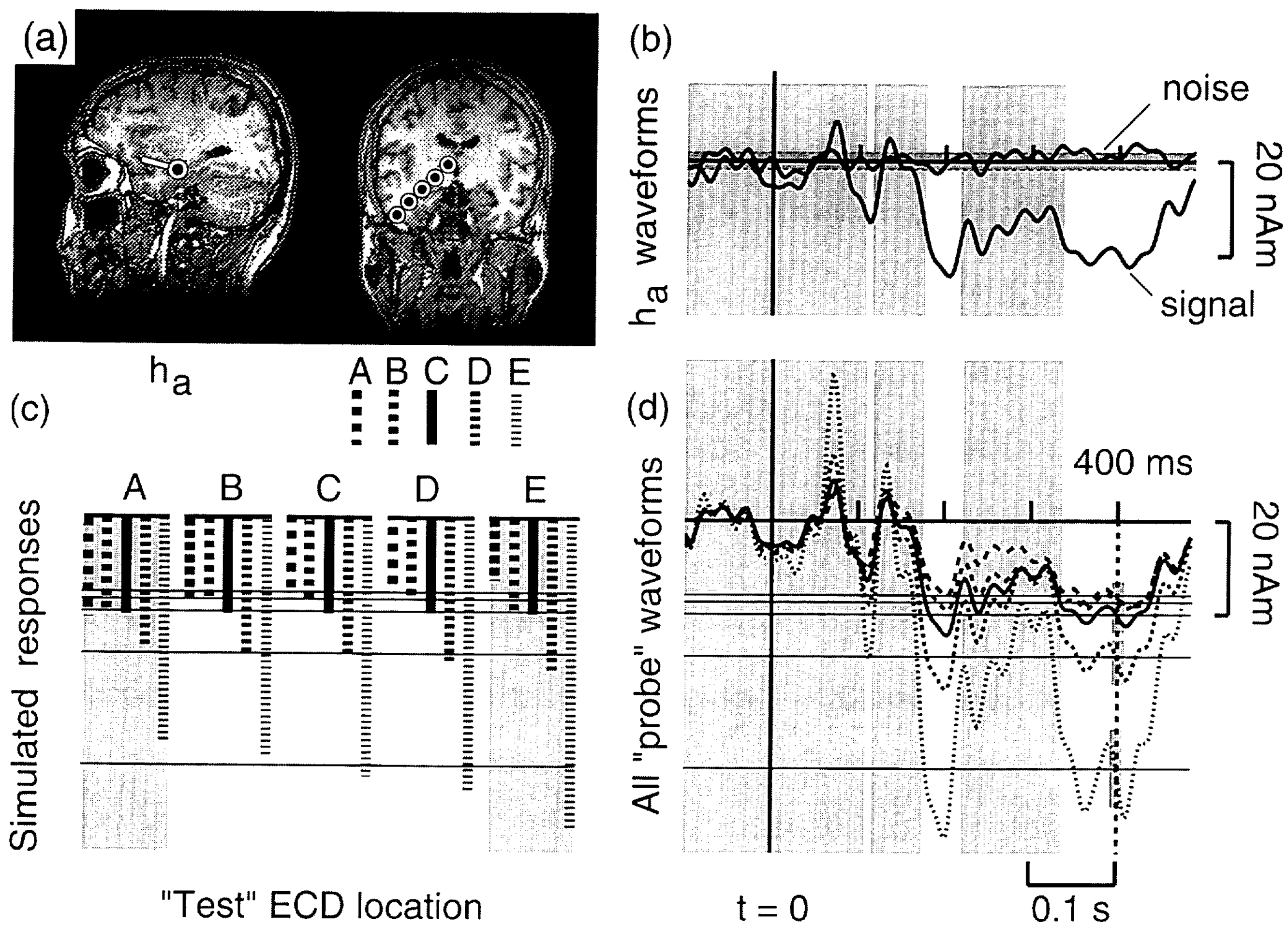

Fig. 4. a: location and orientation of the ECD which characterizes SSP component h_a at site C in the left anterior hippocampus. Additional sites A, B, D and E are displaced radially from C by −2, −1 + 1 and +2 cm, respectively. b: SSP waveforms for component h_a for evoked responses to auditory oddballs (signal) and for data recorded by the array without the subject (noise). The horizontal shaded area indicates the standard deviation $\pm\sigma$ of the noise waveform. c: the amplitudes of SSP waveforms for components determined by a family of 'probe' ECDs located at sites A–E. Responses are shown as vertical bars for data simulated for 'test' ECD sources located at one of the sites A–E with orientation parallel to h_a. The 'probe' locations are indicated by the line type. The 'test' ECD source locations are displayed sequentially on the horizontal axis. Responses for each 'test' source location are normalized to the results for 'probe' h_a. d: SSP waveforms for 'probes' located at sites A–E for evoked responses to the auditory oddballs. The standard deviation $\pm\sigma$ of the noise waveforms determined for each 'probe' is indicated by the short vertical shaded areas at 400 ms. The full-scale vertical shaded areas in b and d indicate epochs with responses which are not within $\pm\sigma$ of the values determined from simulation for an isolated ECD source located at site B, C or D.

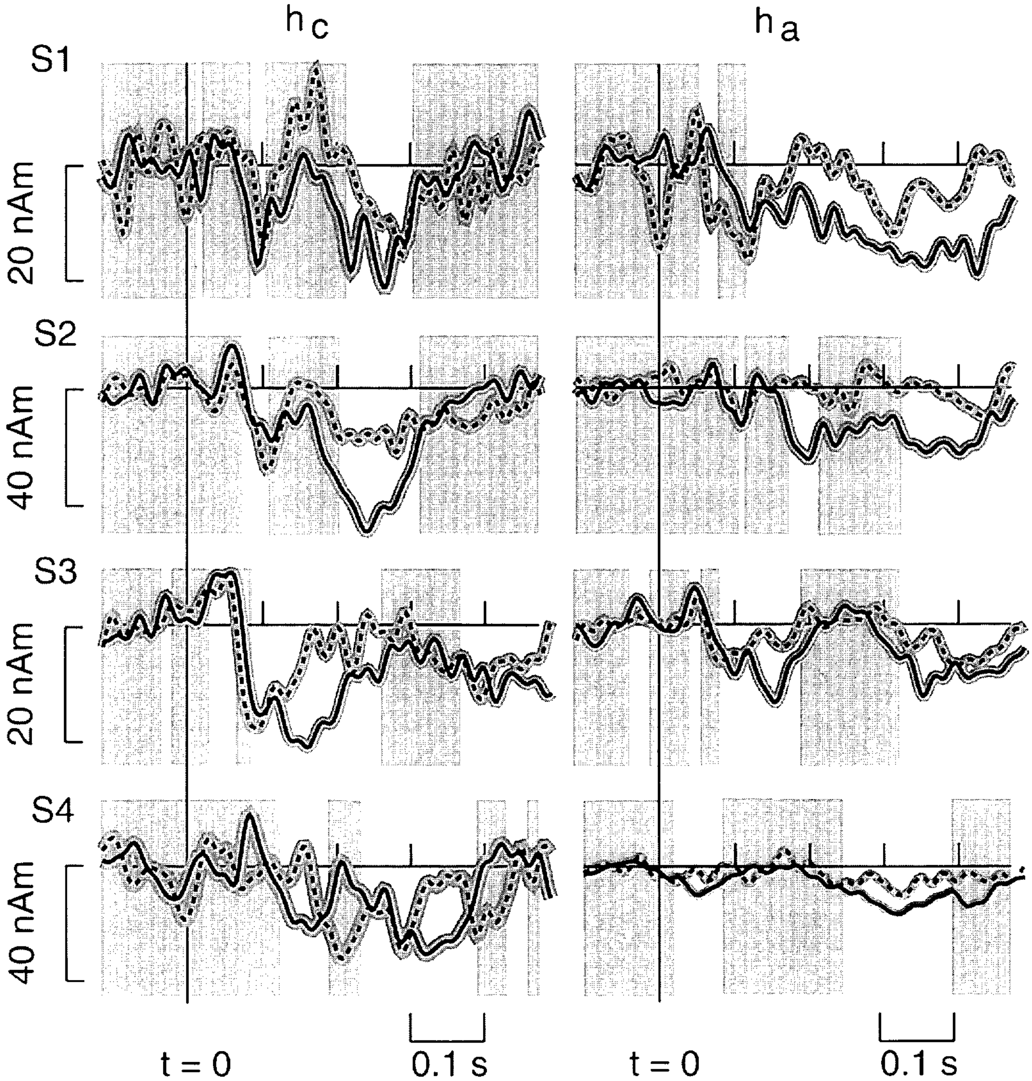

Fig. 5. SSP waveforms for responses to auditory oddball stimuli in the left hippocampus with orientation in the anterior direction (h_a) and in the dorsal–lateral direction in the coronal plane (h_c). The 4 subjects lifted the right index finger on the auditory oddball (solid lines) and passively attended to the stimuli (dashed lines). The shaded areas surrounding each waveform indicate the standard deviations of the system noise. The vertical shaded areas indicate epochs with topographies which are inconsistent with an isolated source within 1 cm of the anterior hippocampus.

activity which is in excess of $\pm\sigma$ of the simulated responses for an ECD parallel to h_a located at either sites B, C or D. Although deflections during the shaded epochs may contain contributions from hippocampal formation activity, more complex source analysis is required to disentangle the generators.

Fig. 5 illustrates the effect of attention on left hippocampal waveforms for anterior–posterior orientation h_a and in the coronal plane h_c in 4 subjects. The system noise for each subject and 'probe' is represented by the shaded thickness of the lines. Epochs which are not consistent with an ECD source located within a radial displacement of 1 cm of site C in anterior hippocampus are indicated by the vertical shaded bars. For example, subject S2 shows a response on the left in hippocampal component h_a but not in component h_c in the 'lift' condition at 400 ms. This is consistent with the topographies shown in Fig. 2 for this subject. The signal-to-noise is poor at this latency for the h_c component and the waveform scaling are dominated by system noise. However, the h_a component shows a clear attentional effect at 400 ms. Both components h_a and h_c contribute at 200 ms.

Although the intrasubject variability is substantial, all subjects show attention-enhanced hippocampal activity in both the h_a and h_c components for some epochs at latencies ranging from 200 to 500 ms. In addition, there is an indication of medial temporal activity between 60 and 100 ms in each subject.

4. Discussion

We observed synchronized postsynaptic activity in medial temporal areas with source strengths of 20–40 nA.

Magnetic fields recorded from transverse guinea pig hippocampal slices have been attributed to effective current dipole moments for pyramidal cell activation of 0.2 pA/cell [15,26]. Production of a dipolar source of several nA would thus require synchronous activation of a population of 10^4 neurons, corresponding to a hippocampal volume of approximately 3 mm^3. It is probable that the coherence of the in vivo neural network is not as high as in an electrically stimulated slice preparation. Thus, the MEG signals may have been generated by coherent activation in medial temporal neuronal population exceeding the minimum volume of 30–60 mm^3.

Most prominent anatomical connections converge to the hippocampal formation via entorhinal cortex from polymodal association areas. The hippocampal formation may be seen as a comparator: it selects the output channels from the polymodal association areas for memory encoding and retrieval [22,35]. In this study, the MEG responses are consistent with neuronal population activity dominated by sources within the temporal lobe at 30–120 ms, followed by prominent attention-dependent hippocampal responses coincident with widespread cortical activity at 200–500 ms. Interestingly, the early signs of activity at 30–120 ms suggest some interaction between auditory areas and hippocampus prior to attention-dependent activity in association cortex. However, practically all the cortical areas projecting to entorhinal cortex have been regarded as polysensory association cortex [11,14]. This is consistent with the strongest hippocampal activity observed between 200 and 500 ms in this study.

In the hippocampal sheet of pyramidal cells, apical dendrites are aligned towards the center of the head, with a more posterior orientation in the anterior area. Main incoming pathways reach the hippocampal formation via entorhinal cortex and terminate to the dendrites in laminar fashion [17]. Selective summation of coherent synaptic activation, possibly synchronized by long-range, cross-regional inhibition [33], has been suggested as a generator of prominent local postsynaptic current flow [6]. The most prominent hippocampal current flow observed in this study between 200 and 500 ms after attended oddball stimuli tended to have contributions from both h_a and h_c, which would correspond to a ventral medial posterior orientation. This orientation is consistent with activity near neuronal pathways which connect anterior hippocampus with the rest of the brain. Moreover, evoked neuronal population activity at these latencies was modulated by the attentional state of the subject in good agreement with results from depth electrode studies of attention-enhanced ERPs [6,20].

5. Conclusions

MEG source analysis assists in bridging the gap between single cell studies and neuronal population activity recorded as field topographies at the scalp. With the current method, MEG arrays may be utilized to reveal the dynamics of both subcortical and cortical neuronal populations. This non-invasive technique opens the possibility of imaging millisecond-scale hippocampal function in intact human brain for comparison with responses obtained during pathological conditions. The clinical importance is evident in the evaluation of disorders which affect memory or damage the hippocampal formation, such as Alzheimer's disease and temporal lobe epilepsy. Moreover, the excellent temporal resolution of MEG measurements makes the identification of both sequential and oscillatory activation of neuronal populations in medial temporal and cortical structures possible during cognitive processing.

Acknowledgements

We thank R. Hari and A. Pääkkönen for comments on the manuscript, M. Seppä for software development and M. Hämäläinen for comments and software for the forward calculations. This study was supported by the Academy of Finland, the Sigrid Jusélius Foundation and a US National Institute of Neurological Disorders and Stroke National Research Service Award. The MRI scans were obtained at the Department of Radiology, Helsinki University Central Hospital.

References

[1] Ahonen, A.I., Hämäläinen, M., Kajola, M., Knuutila, J., Laine, P., Lounasmaa, O., Parkkonen, L., Simola, J. and Tesche, C., 122-channel SQUID instrument for investigating the magnetic signals from human brain, *Physica Scripta*, T49 (1993) 198–205.

[2] Brenner, D., Lipton, J., Kaufman, L. and Williamson, S.J., Somatically evoked fields of the human brain, *Science*, 189 (1978) 81–83.

[3] Donchin, E., Event-related potentials: a tool in the study of human information processing. In: H. Begleiter (Eds.), *Evoked Brain Potentials and Behavior*, Plenum, New York, 1979, pp. 13–88.

[4] Friedman, R. and Goldman-Rakic, P.S., Activation of the hippocampus and dentate gyrus by working memory: a 2-deoxyglucose study of behaving Rhesus monkeys, *J. Neurosci.*, 8 (1988) 4693–4706.

[5] Halgren, E., Baudena, P., Clarke, J., Heit, G., Liégeois, C., Chauvel, P. and Musolino, A., Intracerebral potentials to rare target and distractor auditory and visual stimuli. I. Superior temporal plane and parietal lobe, *Electroencephalogr. Clin. Neurophysiol.*, 94 (1995) 191–220.

[6] Halgren, E., Squires, N.K. and Wilson, C.L., Endogenous potentials generated in the human hippocampal formation and amygdala by infrequent events, *Science*, 210 (1980) 803–805.

[7] Hämäälinen, M., Hari, R., Ilmoniemi, R., Knuutila, J. and Lounasmaa, O.V., Magnetoencephalography – theory, instrumentation, and applications to noninvasive studies of signal processing in the human brain, *Rev. Mod. Phys.*, 65 (1993) 413–497.

[8] Hämäläinen, M. and Sarvas, J., Realistic conductivity geometry model of the human head for interpretation of neuromagnetic data, *IEEE Trans. Biomed. Eng.*, 36 (1989) 165–171.

[9] Helmholtz, H., Uber einige Gesetze der Verteilung elektrischer Ströme in Körperlichen Leitern mit Anwendung auf die trierisch electrischen Versuche, *Ann. Phys. Chem.*, 89 (1853) 211–233, 353–377.

[10] Ilmoniemi, R.J. and Williamson, S.J., Analysis for the magnetic alpha rhythm in signal space, *Soc. Neurosci. Abstr.*, 13 (1987) 46.

[11] Insausti, R., Amaral, D.G. and Cowan, W.M., The entorhinal cortex of monkey: II. Cortical afferents, *J. Comp. Neurol.*, 264 (1987) 356–395.

[12] Ioannides, A.A., Liu, M.J, Liu, L.C., Bamidis, P.D., Hellstrand, E. and Stephan, K.M., Magnetic field tomography of cortical and deep processes: examples of 'real-time mapping' of averaged and single trial MEG signals, *Int. J. Psychophysiol.*, in press.

[13] Johnson, R., Scalp-recorded P300 activity in patients following unilateral temporal lobectomy, *Brain*, 111 (1988) 1517–1529.

[14] Jones, E.G. and Powel, T.P.S., An anatomical study of converging sensory pathways within the cerebral cortex of monkey, *Brain*, 93 (1970) 793–820.

[15] Kyuhou, S. and Okada, Y., Detection of magnetic evoked fields associated with synchronous population activities in the transverse CA1 slice of the guinea pig, *J. Neurophysiol.*, 70 (1993) 2665–2668.

[16] Lewine, J.D., Roeder, S.B., Oakey, M.T., Arthur, D.L., Aine, C.J., George, J.S. and Flynn, E.R., Localization of the generators of the magnetic P3. In: S. Williamson, M. Hoke, G. Stroink and M. Kotani (Eds.), *Advances in Biomagnetism*, Plenum, New York, 1990, pp. 229–238.

[17] Lorente de No, R., Studies on the structure of the cerebral cortex: I. The area entorhinalis, *J. Psychol. Neurol.*, 45 (1934) 381–438.

[18] Lütkenhöner, B., Biomagnetic localization accuracy for single and multiple sources. In *5th International Congress: International Society for Brain Electromagnetic Topography Book of Abstracts*, Westfälische Wilhelms-Universität, Müster, Germany, 1994, pp. 54.

[19] Mazziotta, J.C., Phelps, M.E., Carson, R.E. and Kuhl, D.E., Tomographic mapping of human cerebral metabolism: auditory stimulation, *Neurol.*, 32 (1982) 921–937.

[20] McCarthy, G., Wood, C., Williamson, P. and Spencer, D., Task-dependent field potentials in human hippocampal formation. *J. Neurosci.*, 9 (1989) 4253–4268.

[21] Lewine, J.D., Edgar, J.C., Repa, K., Paulson, K., Astur, R.S. and Orrison, W.W., A physical phantom for simulating the impact of pathology on magnetic source imaging. In: C. Baumgartner, L. Deecke, G. Stroink and S.J. Williamson (Eds.), *Biomagnetism: Fundamential Research and Clinical Applications*, Elsevier, Amsterdam, 1995, pp. 368–372.

[22] Mesulam, M., Large-scale neurocognitive networks and distributed processing for attention, language and memory, *Ann. Neurol.*, 28 (1990) 597–613.

[23] Mishkin, M., Memory in monkeys severely impaired by combined but not by separate removal of amygdala and hippocampus, *Nature*, 273 (1978) 297–298.

[24] Murray, E.A. and Mishkin, M., Severe tactual as well as visual memory deficits follow combined removal of the amygdala and the hippocampus in monkeys, *J. Neurosci.*, 4 (1984) 2565–2580.

[25] Murray, E.A. and Mishkin, M., Amygdalectomy impairs cross-modal association in monkeys, *Science*, 228 (1985) 604–606.

[26] Okada, Y.C., Kaufman, L. and Williamson, S.J., Hippocampal formation as a source of endogenous slow potentials, *Electroencephalogr. Clin. Neurophysiol.*, 55 (1983) 417–426.

[27] Pardo, J.V., Fox, P.T. and Raichle, M.E., Localization of a human system for sustained attention by positron emission tomography, *Nature*, 349 (1991) 61–64.

[28] Polich, J. and Squire, L., P300 from amnesic patients with bilateral hippocampal lesions, *Electroencephalogr. Clin. Neurophysiol.*, 86 (1993) 408–417.

[29] Press, G.A., Amaral, D.G. and Squire, L.R., Hippocampal abnormalities in amnesic patients revealed by high-resolution magnetic resonance imaging, *Nature*, 341 (1989) 54–57.

[30] Rogers, R.L., Baumann, S.B., Papanicolaou, A.C., Bourbon, T.W., Alagarsamy, S. and Eisenberg, H.M., Localization of the P3 sources using magnetoencephalography and magnetic resonance imaging, *Electroencephalogr. Clin. Neurophysiol.*, 79 (1991) 308–321.

[31] Rolls, E.T., Parallel distributed processing in the brain: implications of the functional architecture of neuronal networks in the hippocampus. In: R.G.M. Morris (Ed.), *Parallel Distributed Processing. Implications for Psychology and Neurobiology*, Clarendon Press, Oxford, 1989, pp. 286–308.

[32] Scoville, W.B. and Milner, B., Loss of recent memory after bilateral hippocampal lesions, *J. Neurol. Neurosurg. Psychiatry*, 20 (1957) 11–21.

[33] Sik, A., Ylinen, A., Penttonen, M. and Buzsaki, G., Inhibitory CA1–CA3–Hilar region feedback in the hippocampus, *Science*, 265 (1994) 1722–1724.

[34] Squire, L.R., Memory and the hippocampus: a synthesis from findings with rats, monkeys, and humans, *Psychol. Rev.*, 99 (1992) 195–231.

[35] Squire, L.R. and Zola-Morgan, S., The medial temporal lobe memory system, *Science*, 253 (1991) 1380–1386.

[36] Stapelton, J.M. and Halgren, E., Endogenous potentials evoked in simple cognitive tasks: depth components and task correlates, *Electroencephalogr. Clin. Neurophysiol.*, 67 (1987) 44–52.

[37] Tesche, C. and Karhu, J., Signal-space analysis with forward modelling reveals task-dependence in hippocampal source areas. In: *5th International Congress: International Society for Brain Electromagnetic Topography Book of Abstracts*, Westfälische Wilhelms-Universität, Münster, Germany, 1994, pp. 178–179.

[38] Tesche, C.D., Uusitalo, M.A., Ilmoniemi, R.J., Huotilainen, M., Kajola, M. and Salonen, O., Signal-space projections of MEG data characterize both distributed and well-localized neuronal sources, *Electroencephalogr. Clin. Neurophysiol.*, 95 (1995) 189–200.

[39] Tulving, E. and Schachter, D., Priming and human memory systems, *Science*, 247 (1990) 301–306.

[40] Uusitalo, M.A., *Projection Method in Magnetoencephalography*. M.Sc. thesis, Helsinki University of Technology, 1993 (in Finnish).

[41] Vinogradova, O.S., The hippocampus and the orienting reflex. In: E.N. Sokolov, O.S. Vinogradova (Eds.), *Neuronal Mechanisms of the Orienting Reflex*, Lawrence Erlbaum, New Jersey, 1975, pp. 128–154.

[42] Yamaguchi, S. and Knight, R.T., Anterior and posterior association cortex contributions to the somatosensory P300, *J. Neurosci.*, 11 (1991) 2039–2054.

[43] Zola-Morgan, S., Squire, L.R., Amaral, D.G. and Suzuki, W.A., Lesions of the parahippocampal cortex that spare the amygdala and hippocampal formation produce severe memory impairment, *J. Neurosci.*, 9 (1989) 4355–4370.